

Robust control of quantum gates via sequential convex programming

Robert L. Kosut*

SC Solutions, Inc., 1261 Oakmead Parkway, Sunnyvale, CA 94085

Matthew D. Grace[†] and Constantin Brif[‡]

Department of Scalable & Secure Systems Research, Sandia National Laboratories, Livermore, CA 94550

(Dated: May 5, 2022)

Resource tradeoffs can often be established by solving an appropriate robust optimization problem for a variety of scenarios involving constraints on optimization variables and uncertainties. Using an approach based on sequential convex programming, we demonstrate that a substantial fidelity robustness is obtainable against uncertainties while simultaneously using limited resources of control amplitude and bandwidth. What is required is a specific knowledge of the range and character of the uncertainties, a process referred to in the control theory literature as “uncertainty modeling.” Using a general one-qubit model for illustrative simulations of a controlled qubit, we generate robust controls for a universal gate set. Our results demonstrate that, even for this simple model, there exist a rich variety of control design possibilities.

I. INTRODUCTION

Robust control and robust optimization of uncertain systems are essential in many areas of science and engineering [1–7]. Recently, there has been much interest in achieving robust control of quantum information systems in the presence of uncertainty [8–39]. An important property of quantum information processing that distinguishes it from most other applications is the requirement of an unprecedented degree of precision in controlling the system dynamics. Also, due to the very fast timescale of physical processes in the quantum realm, implementing closed-loop feedback control is extremely difficult and thus open-loop control arises as the most feasible option in most circumstances.

For quantum information systems, a robust optimization problem can be formulated as a search for *design variables* θ that maximize a measure of *quantum gate fidelity* \mathcal{F} over a range of *uncertain parameters* δ (i.e., $\delta \in \Delta$, where Δ is the *uncertainty set*). Fidelity compares a target unitary transformation against the actual quantum channel which is dependent on both θ and δ . Fidelity is typically normalized: $0 \leq \mathcal{F} \leq 1$, and the maximum value $\mathcal{F} = 1$ corresponds to a perfect generation of the target transformation. The design variables θ can include time-dependent control fields (for both open-loop and closed-loop control), measurement configurations (usually, for closed-loop feedback control), constants associated

with physical implementation, the circuit lay-out, and so on. The uncertainties in δ can affect any elements of the system Hamiltonian (including the design variables), with specific manifestations and ranges depending on details of the physical implementation and external hardware. For example, uncertainties can represent dispersion and/or slow time variation of parameters such as coupling strengths, exchange interactions, and applied electromagnetic fields, as well as additive and/or multiplicative noise in control fields. The uncertainty set Δ can thus, in general, combine deterministic and random variables. Whatever the case, we assume that both θ and δ are constrained to known sets Θ and Δ , respectively.

One common approach to robust control of quantum gates (e.g., see Ref. [20]) is based on maximizing the average fidelity given by

$$\mathcal{F}_{\text{avg}}(\theta) = \mathbf{E}_{\delta \in \Delta} \{ \mathcal{F}(\theta, \delta) \}, \quad (1)$$

where $\mathcal{F}(\theta, \delta)$ denotes the fidelity as a function of design and uncertain variables, and $\mathbf{E}_{\delta \in \Delta} \{ \cdot \}$ is expectation with respect to the underlying distribution in Δ . Often the average fidelity is well approximated as the sum over a discrete sample and associated probabilities $\{ \delta_i \in \Delta, p_i, \forall i \}$, i.e., $\mathcal{F}_{\text{avg}}(\theta) = \sum_i p_i \mathcal{F}(\theta, \delta_i)$. While this approach is applicable in some cases (in particular, when the uncertainty represents weak random noise), the stringent performance requirements of quantum information processing make it more appropriate, in general, to estimate gate errors by using a *worst-case fidelity* measure with respect to all uncertainties $\delta \in \Delta$,

$$\mathcal{F}_{\text{wc}}(\theta) = \min_{\delta \in \Delta} \mathcal{F}(\theta, \delta). \quad (2)$$

*Electronic address: kosut@scsolutions.com

[†]Electronic address: mgrace@sandia.gov

[‡]Electronic address: cnbrif@sandia.gov

Also, *worst-case robust optimization* (or *minimax optimization*) is a well known approach employed in many classical problems [7, 40–55], and some of the methods developed for these applications can be adapted for robust control of quantum gates. The worst-case robust optimization problem for quantum gate fidelity is formulated as:

$$\begin{aligned} & \text{maximize} \quad \min_{\delta} \mathcal{F}(\theta, \delta) \\ & \text{subject to} \quad \theta \in \Theta, \delta \in \Delta \end{aligned} \quad (3)$$

The goal reflected in (3) is to find the design variables $\theta \in \Theta$ that maximize the worst-case fidelity (2).

In control applications, the design set Θ represents the set of control constraints. Θ is most often convex or sufficiently well approximated by a convex set. In some cases so is the uncertainty set Δ , although even if it is not that is not the principal obstacle to solving (3). What makes the problem difficult is that the fidelity measure is not a convex function of θ for any sample $\delta \in \Delta$. Non-convex optimization problems are common in all of science and engineering and have engendered numerous numerical approaches to finding local optimal solutions. In particular, effective methods have been developed in recent years for worst-case robust optimization with non-convex cost functions [50–56].

In optimal control applications, the functional dependence of the objective (e.g., fidelity) on the control variables is referred to as the *optimal control landscape* [57–60]. For an ideal model of a closed quantum system with no uncertainties, the optimal control landscape for the generation of unitary transformations has a very favorable topology. Specifically, provided a number of physically reasonable conditions are satisfied, the landscape is free of local optima, i.e., there exist one manifold of global minimum solutions (resulting in $\mathcal{F} = 0$) and one manifold of global maximum solutions (resulting in $\mathcal{F} = 1$), while all other extrema reside on saddle-point manifolds [61–63]. Such a favorable landscape topology facilitates easy optimization, as any gradient-based search is guaranteed to reach the global maximum [64]. Unfortunately, when uncertainties are present, this landscape topology is not preserved. Typically, uncertainties cause the drop and fragmentation of the global maximum manifold, resulting in the emergence of multiple local maxima [39] (the landscape also undergoes a similar transformation when control fields are severely constrained [65]). Provided that the range of uncertainty is not too large, many of these local optimal solutions will have fidelities close to one.

For quantum information systems, there is considerable ongoing effort to develop efficient methods for obtaining a good

solution to the problem of robust control, for either average or worst-case fidelity. The majority of existing approaches rely on a numerical optimization procedure, mostly involving a gradient-based search for maximizing the average fidelity of Eq. (1). In some cases, a randomized search such as a genetic algorithm is employed [39]. The results demonstrate the existence of many solutions with high fidelities, consistent with the control landscape picture discussed above. Additionally, the optimal controls are often similar to the corresponding initial controls, provided the latter are reasonably good. This phenomenon, also observed in many engineering and design applications employing local search algorithms, supports the need for developing tools to efficiently calculate a good initial control. In particular, empirical evidence and simulations suggest that robust controls for an uncertain quantum system can be found by searches that start from solutions generated by applying *optimal control theory* or *dynamical decoupling* to the ideal (zero-uncertainty) counterpart system (see, e.g., [60], [38] and the references therein).

In this paper, we propose the use of *sequential convex programming* (SCP) which is one of several methods available for numerically solving optimization problems like (3). (See [66] for a collection of earlier SCP varieties and uses and [67] for a recent informative overview.) SCP provides a framework for finding local optimal solutions to the general robust optimization problem (3). The specific SCP algorithm used here, delineated in (4) below, follows directly from [51, 54]. It was used previously for robust design of slow-light tapers in photonic-crystal waveguides [54, 55] and quantum potential profiles for electron transmission in semiconductor nanodevices [56]. In this paper, we apply this SCP algorithm to identify robust control fields for generation of quantum gates in an uncertain one-qubit system.

II. SEQUENTIAL CONVEX PROGRAMMING

The SCP algorithm used here is shown in abstract form in (4). The algorithm must be initialized with (i) a control in the feasible set Θ , which is assumed to be convex, (ii) samples $\delta_{i,1} = 1, \dots, L$ taken from the uncertainty set Δ , which need not be convex, and (iii) selecting the initial size of a convex trust region $\tilde{\Theta}_{\text{trust}}$. The trust region is selected so that the linearized fidelity used in the optimization step retains sufficient accuracy. In each iteration the SCP algorithm returns the optimal increment $\tilde{\theta}$ and the associated worst-case (linearized) fidelity. To compute the actual worst-case fidelity requires

simulating the system with the control variables $\theta + \tilde{\theta}$ as indicated in Step 3 of (4). The centerpiece is the optimization step which, in the version shown (4) is gradient based, thereby resulting in L affine constraints in $\tilde{\theta}$, and hence is a convex optimization. The Hessian, perhaps not so easily computed, is easily added as shown in Appendix A. In some cases the number of samples, L , can be very large. Fortunately, however, computational complexity grows gracefully with the number of constraints and thus does not grossly effect the convex optimization efficiency [68].

Robust control via SCP (4)

Initialize

initialize control $\theta \in \Theta \subseteq \mathbf{R}^N$
sample uncertainties/noises $\delta_i \in \Delta$, $i = 1, \dots, L$
set size of trust region $\tilde{\Theta}_{\text{trust}} \subseteq \mathbf{R}^N$

Repeat

1. Calculate fidelities and gradients

$$\mathcal{F}(\theta, \delta_i), \nabla_{\theta} \mathcal{F}(\theta, \delta_i) \in \mathbf{R}^N, i = 1, \dots, L$$

2. Using the linearized fidelity, solve for the increment $\tilde{\theta}$ from the convex optimization:

$$\begin{aligned} &\text{maximize} \quad \min_{i=1, \dots, L} \mathcal{F}(\theta, \delta_i) + \nabla_{\theta} \mathcal{F}(\theta, \delta_i)^T \tilde{\theta} \\ &\text{subject to} \quad \theta + \tilde{\theta} \in \Theta, \tilde{\theta} \in \tilde{\Theta}_{\text{trust}} \end{aligned}$$

3. Update

If $\min_{i=1, \dots, L} \mathcal{F}(\theta + \tilde{\theta}, \delta_i) > \min_{i=1, \dots, L} \mathcal{F}(\theta, \delta_i)$

Then $\theta \leftarrow \theta + \tilde{\theta}$

increase size of trust region $\tilde{\Theta}_{\text{trust}}$

Else decrease size of trust region $\tilde{\Theta}_{\text{trust}}$

Until Stopping criteria satisfied

In §A we show how the gradient and/or Hessian forms can be cast in standard forms compatible with freely available software specifically designed to solve such convex optimization problems. In general, solving the convex optimization step is not the most time consuming step in the SCP algorithm. The time-burden in each iteration falls more often on the simulations required to obtain the fidelities and gradients (and the Hessian if used) at each uncertainty sample. Of course as is the case with numerically computing anything to do with a quantum information system, there always lurks the “curse of dimensionality”, *i.e.*, exponential scaling with the number of qubits.

Despite many advantages, SCP is a local optimization method. As such there is no way to verify that an optimal solution has been found. In the case of maximizing fidelity, which by construction cannot exceed one, it would seem that at least the maximum is known, so if $\mathcal{F} = 1$ is achieved, it is an optimal solution. However, in many cases we see fidelities that are extremely close to one, *e.g.*, $\log_{10}(1 - \mathcal{F}) \in [-6, -4]$. Although 4 to 6 nines following the decimal point is 1 for most engineering problems, for quantum computing every additional nine can greatly decrease the spatial and temporal resources required for fault-tolerant operation. Ergo, here $1 \neq 1!$

III. SEQUENTIAL CONVEX PROGRAMMING FOR AN UNCERTAIN QUBIT

In this section we show how to use SCP (4) for some common uncertainty and control generation and constraint scenarios. We focus on controlling a single qubit system with Hamiltonian,

$$H(t) = c(t)\omega_x X + \omega_z Z, 0 \leq t \leq T \quad (5)$$

where $c(t)$ is the external control field and X, Z are the respective Pauli matrices. The parameters ω_x and ω_z are constant but uncertain over the time interval $[0, T]$. In regard to (3), we can equate the uncertain parameters δ with (ω_x, ω_z) .

A. Control generation and constraints

The control $c(t)$ is typically the output of a signal generation device whose dynamics impose constraints on magnitudes, bandwidth, and so on. To illustrate the use of SCP we make the simplifying assumption that the control is piecewise-constant over N uniform time intervals of width T/N , *i.e.*, for $k = 1, \dots, N$,

$$c(t, \theta) = \theta_k \text{ and } (k-1)T/N \leq t < kT/N, \quad (6)$$

Constraints due to signal generation dynamics are explored in §B. In general the set Θ in (3) reflects the control constraints. Consider, for example, Table I, showing many typical restrictions on the control.

This list of control constraints is certainly not exhaustive. However, since $c(t, \theta)$ is a linear function of θ (6), then these, or any combinations, form convex constraints on $\theta \in \mathbf{R}^N$. For example, with the strictly piece-wise-constant control (6) the

Constraint	Set Θ
none	\mathbf{R}^N
fluence	$\int_0^T c^2(t, \theta) dt \leq \gamma$
magnitude	$c^{\min} \leq c(t, \theta) \leq c^{\max}, t \in [0, T]$
slew rate	$ \dot{c}(t, \theta) \leq \beta, t \in [0, T]$
area	$\int_0^T c(t, \theta) dt \leq \alpha$
linear	$A\theta = b$

TABLE I: Typical control constraints.

fluence constraint becomes $(T/N)\|\theta\|_2^2 \leq \gamma^2$. The bounding parameters in Table I can also be used as design variables to establish control resource tradeoffs via SCP. This is explored further in § V for fidelity vs. fluence.

B. Fidelity

For the single-qubit system (5), we use the fidelity,

$$\mathcal{F}(\theta, \omega_x, \omega_z) = |\text{Tr}(V^\dagger U_T)/2|^2 \quad (7)$$

This fidelity, normalized to $[0, 1]$, is a measure of the *phase-independent* alignment between the desired unitary logic gate V and the actual unitary operator U_T attained at the final time T . Applying the piece-wise-constant control (6) to the Hamiltonian (5) gives,

$$U_T = \prod_{k=1}^N \exp \left\{ -i \frac{T}{N} (\theta_k \omega_x X + \omega_z Z) \right\} \quad (8)$$

C. Uncertainty modeling

One general approach to modeling the uncertainty in the Hamiltonian parameters (ω_z, ω_x) is via the set describing a *deterministic uncertainty*,

$$\Delta = \{ \|W(\omega - \bar{\omega})\|_\nu \leq 1 \} \quad (9)$$

with parameter vector $\omega = [\omega_x, \omega_z]^T$, nominal values $\bar{\omega} = [\bar{\omega}_x, \bar{\omega}_z]^T$, W a positive definite weighting matrix (here 2×2), and ν typically 2 or ∞ . If $\nu = \infty$ and W is diagonal, then ω_x and ω_z are not correlated, in which case (9) is equivalent to,

$$\Delta = \{ \omega_x^{\min} \leq \omega_x \leq \omega_x^{\max}, \omega_z^{\min} \leq \omega_z \leq \omega_z^{\max} \} \quad (10)$$

If W is not diagonal, then ω_x and ω_z are correlated, possibly arising, respectively, from an approximation of a joint Gaussian or uniform distribution, with W , typically, the inverse of

the covariance matrix associated with a specified confidence region for the parameters.

The uncertainty in the parameters can often be best described via a *probabilistic uncertainty*, e.g.,

$$\Delta = \{ \mathbf{E} \{ \omega \} = \bar{\omega}, \mathbf{E} \{ (\omega - \bar{\omega})(\omega - \bar{\omega})^T \} = R \} \quad (11)$$

where $\mathbf{E} \{ \dots \}$ is with respect to the underlying probability distribution of ω . If that is gaussian, then $\Delta = \{ \omega \in \mathcal{N}(\bar{\omega}, R) \}$.

Uncertainty also arises from noise in the control and other environmental sources, best represented by *stochastic uncertainty*, e.g.,

$$\Delta = \{ \mathbf{E} \{ \omega(t) \} = \bar{\omega}, \mathbf{E} \{ (\omega(t) - \bar{\omega})(\omega(t') - \bar{\omega})^T \} = R(t, t') \} \quad (12)$$

Although (9) is a convex set, as already mentioned, uncertainty modeling sets for SCP need not be convex, e.g., (11) and (12). Step 2 in (4) only requires that the uncertain parameters be *sampled* from the uncertainty set. In our example to follow with uncertainty set (10) we use a simple uniform sampling. More sophisticated variants cycle through a sampling in the optimization step followed by validation on a different sampled set; bad parameters revealed in the validation step can be used in a new sampling for a repeat of the optimization step, e.g., [51].

D. Robust optimization

Gathering the previous pieces together we can form the following instance of (3) for finding a robust control for a single qubit system by solving for the control magnitudes $\theta \in \mathbf{R}^N$ from,

$$\begin{aligned} & \text{maximize} && \min_{\omega_x, \omega_z \in \Delta} \mathcal{F}(\theta, \omega_x, \omega_z) \\ & \text{subject to} && U_T \text{ from (8)} \\ & && \theta \in \Theta \text{ from a combination of sets in Table I} \\ & && (\omega_z, \omega_x) \in \Delta \text{ from (9), (11), or (12)} \end{aligned} \quad (13)$$

Since Θ is a convex set and samples are taken from Δ to form the gradients (and possibly the Hessians), then Step 2 of (4) will be a convex optimization.

IV. ROBUST ONE-QUBIT UNITARY OPERATIONS

We use our SCP routine to construct control fields corresponding to the following set of one-qubit unitary operations

that are robust to variations in ω_x and ω_z :

$$V_I = \begin{bmatrix} 1 & 0 \\ 0 & 1 \end{bmatrix}, V_H = \frac{1}{\sqrt{2}} \begin{bmatrix} 1 & 1 \\ 1 & -1 \end{bmatrix}, V_P = \begin{bmatrix} 1 & 0 \\ 0 & e^{i\pi/4} \end{bmatrix}. \quad (14)$$

Here, V_I , V_H , V_P , correspond to identity, Hadamard, and phase gates, respectively. Note that V_H and V_P represent a universal gate set for one-qubit operations. The uncertainty set considered for all optimizations in this section is

$$\Delta = \{\omega_x \in [0.99, 1.01], \omega_z \in [1.8, 2.2]\}, \quad (15)$$

corresponding to 1% control amplitude uncertainty and 10% drift magnitude uncertainty. In each case, SCP is used to solve for $\theta \in \mathbf{R}^N$ from:

$$\begin{aligned} & \text{maximize} && \min_{(\omega_x, \omega_z) \in \Delta} \mathcal{F}(\theta, \omega_x, \omega_z) \\ & && = \min_{(\omega_x, \omega_z) \in \Delta} |\text{Tr}(V^\dagger U_T)/2|^2 \\ & \text{subject to} && U_T \text{ obtained from (8)} \\ & && \theta \in \mathbf{R}^N \text{ (unconstrained)} \\ & && (\omega_z, \omega_x) \in \Delta \text{ from (15)} \end{aligned} \quad (16)$$

This is solved for all combinations of V_α , where $\alpha \in \{I, H, P\}$, and $T \in \{1, 2, 4\}$, with select elements of $N \in \{5, 10, 20, 80\}$. For all of the results discussed in this section, the initial SCP controls $c^{(0)}$ were optimized for unitary targets of the *nominal* Hamiltonian system

$$\bar{H}(t) = c(t)\bar{\omega}_x X + \bar{\omega}_z Z \quad (17)$$

(where $\bar{\omega}_x$ is the *average* value of ω_x), such that $\mathcal{F}(c^{(0)}, \bar{\omega}_x, \bar{\omega}_z) \leq 0.999$, i.e., $c^{(0)}$ is at best a nearly-optimal control field for the nominal system. Figure 1 presents the resulting control fields and corresponding fidelities. Properties of the robust controls are presented in table II. There are eight configurations of N and T for each unitary target, representing different combinations of N and T . With this one-qubit system and the uncertainty set Δ (15), controls with worst-case fidelities $\mathcal{F}_{\text{wc}} \geq 0.9999$ are obtained for $N \geq 10$ and $T \geq 2$ for all target operations. These results demonstrate that robust, high-fidelity control is possible with a relatively small number of control variables N , provided that the final time T is chosen properly.

Interestingly, the worst-case fidelity for the identity gate actually decreases as the number of time intervals increases from $N = 10$ to $N = 20$ for $T = 2$. This result suggests that the objective function in eq. (16) may possess local sub-optimal critical points, given that the set of controls with $N = 10$ and $T = 2$ is a proper subset of controls with $N = 20$ and

Target operation: Identity

N	T	$\log_{10}(1 - \mathcal{F}_{\text{wc}})$	$\log_{10}(1 - \mathcal{F}_{\text{av}})$	$\Phi[c]$	$\max[c]$
5	1	-3.13	-3.82	103.63	16.21
5	2	-2.35	-3.16	37.24	7.25
10	1	-3.28	-4.20	58.45	11.88
10	2	-5.23	-5.79	51.00	6.59
20	1	-3.31	-4.24	53.66	13.47
20	2	-4.35	-4.98	25.34	6.03
10	4	-4.62	-5.66	28.96	4.22
80	4	-5.08	-5.60	31.74	6.00

Target operation: Hadamard

N	T	$\log_{10}(1 - \mathcal{F}_{\text{wc}})$	$\log_{10}(1 - \mathcal{F}_{\text{av}})$	$\Phi[c]$	$\max[c]$
5	1	-2.20	-3.08	32.27	7.59
5	2	-3.02	-3.74	16.35	3.77
10	1	-2.17	-3.05	36.93	8.02
10	2	-4.33	-4.80	30.33	8.95
20	1	-2.17	-3.06	34.38	8.64
20	2	-4.34	-4.86	30.07	9.17
10	4	-4.06	-4.63	16.60	2.86
80	4	-4.69	-5.12	25.61	5.48

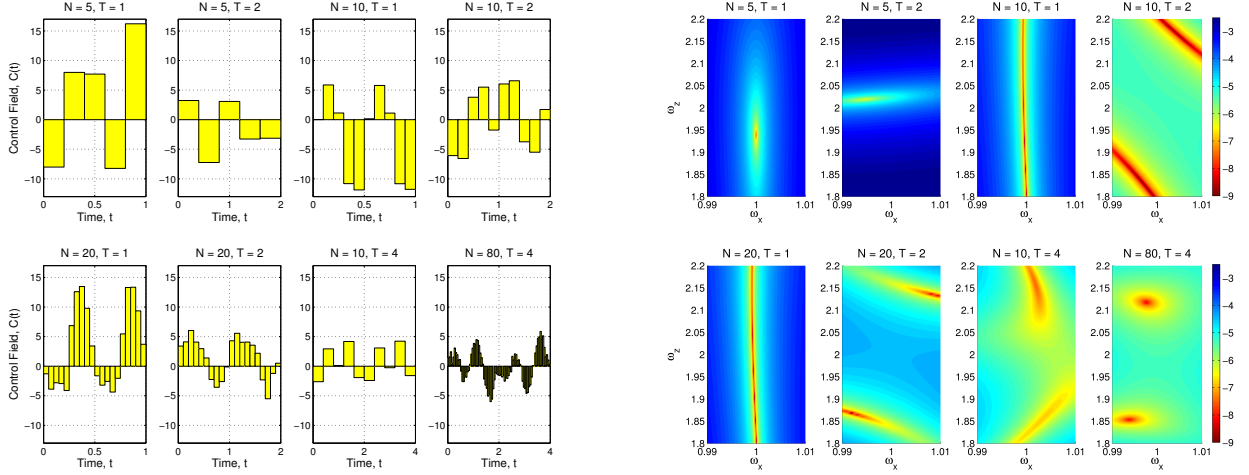
Target operation: Phase

N	T	$\log_{10}(1 - \mathcal{F}_{\text{wc}})$	$\log_{10}(1 - \mathcal{F}_{\text{av}})$	$\Phi[c]$	$\max[c]$
5	1	-2.77	-3.51	41.98	8.39
5	1	-3.71	-4.19	29.99	6.70
10	1	-2.96	-3.55	116.17	28.62
10	2	-4.34	-4.88	25.40	6.80
20	1	-3.02	-3.61	136.06	33.88
20	2	-4.30	-4.77	23.39	7.12
10	4	-5.57	-6.02	46.82	5.87
80	4	-6.00	-6.34	33.51	5.91

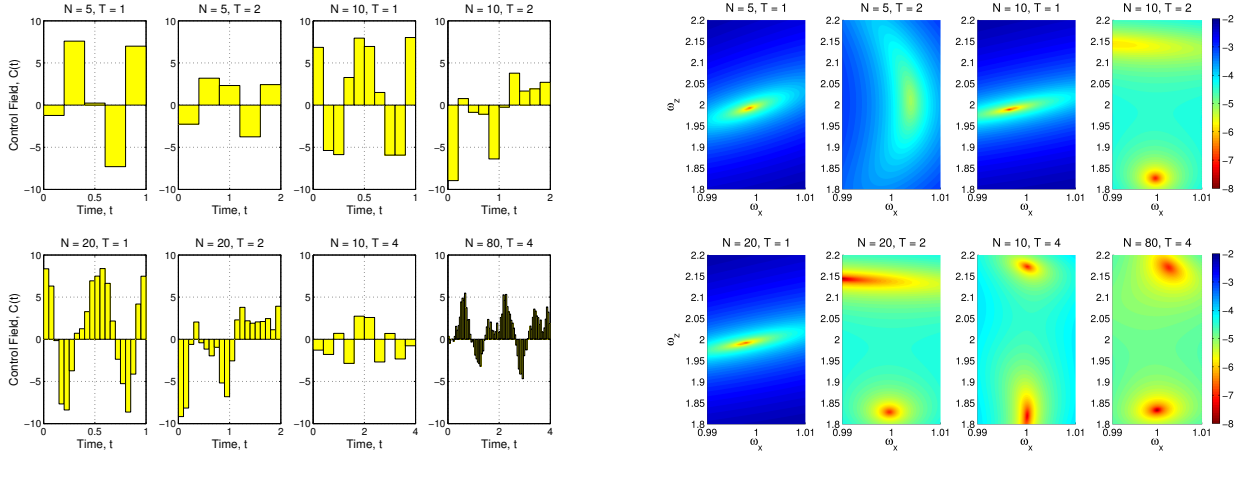
TABLE II: Properties of controls $c(t, \theta)$ for robust one-qubit operations. Here, for the piece-wise-constant robust control from (13) $\Phi[c] = \int_0^T c^2(t, \theta) dt = (T/N) \|\theta\|_2^2$, corresponding to control field fluence, and $\max[c] = \|\theta\|_\infty$ for maximum control magnitude.

$T = 2$. For $T = 1$, the worst-case fidelity for the Hadamard gate also decreases as the number of time intervals increases from $n = 5$ to $N = 20$.

(a) Control & fidelities for identity gate



(b) Control & fidelities for Hadamard gate



(c) Control & fidelities for phase gate

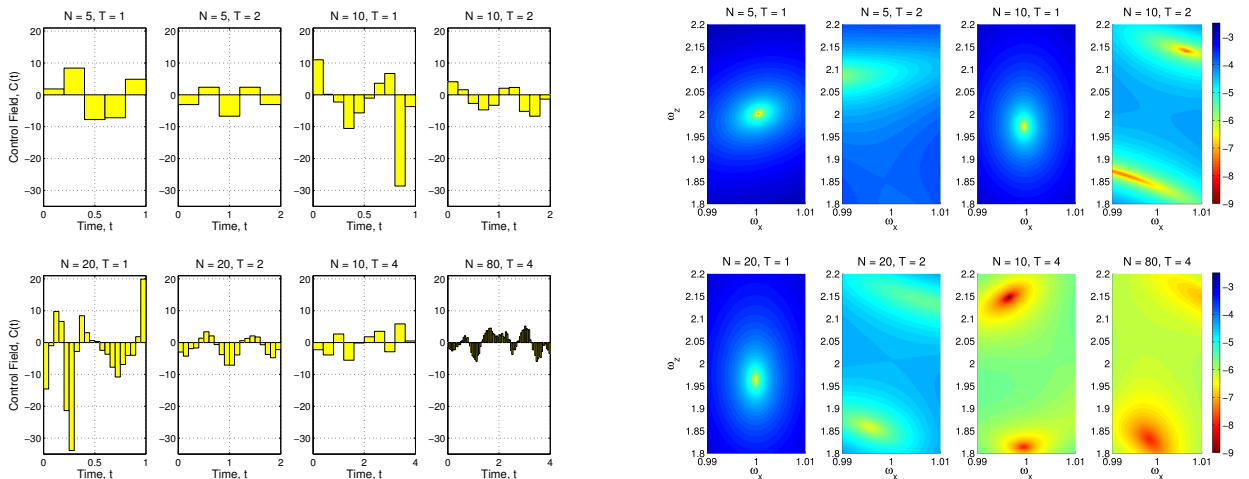


FIG. 1: Optimized control fields and corresponding fidelities for robustness to uncertainty ($\{\omega_x \in [0.99, 1.01], \omega_y \in [1.8, 2.2]\}$) and for several different time intervals (N) and final times (T). (a) identity gate, (b) Hadamard gate, (c) phase gate.

V. GATE FIDELITY VERSUS CONTROL FLUENCE

As a further illustration of the utility of SCP, we solve (13) with a constraint on control fluence and uncertainty in (ω_x, ω_z) in (5) for a target unitary of identity, $V = I_g$, operation time $T = 2$, and with the number of pulses $N = 10$. We solve this constrained optimization problem for a range of bounds on the fluence, denoted by γ , and for two uncertainty sets: Δ from (15) and a nominal case, Δ_0 , effectively no uncertainty,

$$\Delta_0 = \{\omega_z = 2, \omega_x = 1\} \quad (18)$$

Specifically, SCP is used to solve for $\theta \in \mathbf{R}^{10}$ from:

$$\begin{aligned} & \text{maximize} && \min_{(\omega_x, \omega_z) \in \Delta} \mathcal{F}(\theta, \omega_x, \omega_z) \\ & && = \min_{(\omega_x, \omega_z) \in \Delta} |\text{Tr}(V^\dagger U_T)/2|^2 \\ & \text{subject to} && U_T \text{ obtained from (8)} \\ & && \Phi(\theta) = (T/N)\|\theta\|_2^2 \leq \gamma^2 \text{ for varying } \gamma \\ & && (\omega_z, \omega_x) \in \{\Delta_0, \Delta\} \text{ from (18) and (15)} \end{aligned} \quad (19)$$

For each uncertainty set $\{\Delta_0, \Delta\}$ we start the SCP with the previously obtained robust control obtained from (13) for uncertainty set Δ (see the $N = 10, T = 2$ plots in Fig. 1. The initial fluence constraint is set to $\gamma = \infty$, *i.e.*, no control constraint. We subsequently set γ to 0.95 of the fluence of the resulting control ($\Phi(\theta) = (T/N)\|\theta\|_2^2$ with $T/N = 0.2$) found from the SCP routine and repeat the process, starting again with the previous initial control, reduced proportionally to the new fluence constraint, and so on.

In Fig. 2, the solid blue and dotted red lines show, respectively, the resulting tradeoffs between worst-case fidelity error $\log_{10}(1 - \min_{(\omega_z, \omega_x) \in \Delta} \mathcal{F})$ and *achieved* control fluence $(T/N)\|\theta\|_2^2$ for Δ_0 (18) and Δ (15). The dashed blue plot shows the effect of the full uncertainty Δ on each of the respective optimized control fields obtained for the no-uncertainty set Δ_0 as the fluence constraint is lowered. (Note that since we start with $\gamma = \infty$, *i.e.*, no constraint, it follows that the right most points on each line correspond to unconstrained controls.) The wiggly part of the solid blue plot for Δ_0 is strictly due to the SCP stopping criterion: iterations halt if either $\log_{10}(1 - \mathcal{F}) < -16$ or changes in $\log_{10}(1 - \mathcal{F})$ are smaller than 10^{-9} . It is important to note that it is not known if any of the points shown here are elements of a *Pareto front* for fidelity error versus fluence.

Fig. 2 reveals some interesting, and initially surprising features. First, we see extreme sensitivity of the control optimized for the nominal parameter values Δ_0 (solid blue) when

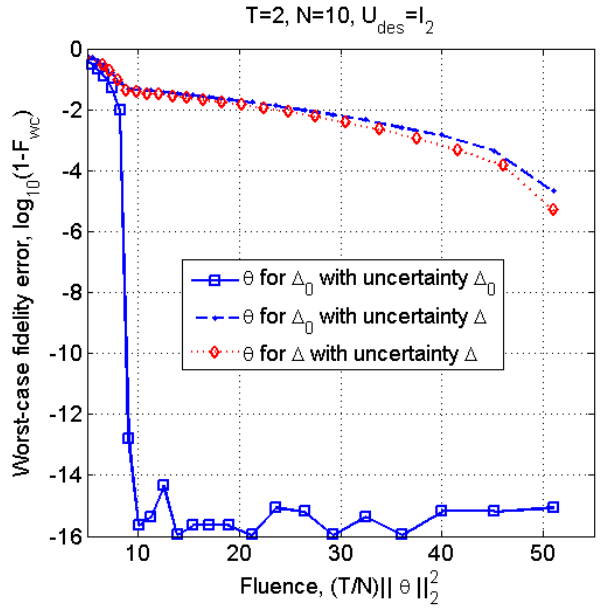


FIG. 2: Worst-case fidelity error $\log_{10}(1 - \mathcal{F}_{wc})$ versus control fluence $\Phi(\theta) = (T/N)\|\theta\|_2^2$ from (19) for the identity gate I_g . For θ optimized for Δ_0 (18), solid blue shows evaluation with Δ_0 , and dashed blue shows evaluation with Δ (15). For θ optimized for Δ , dotted red shows evaluation for Δ .

evaluated over the full uncertainty range Δ (dashed blue). Specifically, at the right most points on the tradeoff curves, the latter control obtained from (19), denoted by θ_Δ and the former, denoted by θ_{Δ_0} , are given by,

$$\theta_\Delta = \begin{bmatrix} -6.078 \\ -6.557 \\ 3.794 \\ 5.502 \\ -1.756 \\ 6.044 \\ 6.587 \\ -3.753 \\ -5.507 \\ 1.722 \end{bmatrix}, \quad \theta_{\Delta_0} = \begin{bmatrix} -6.075 \\ -6.554 \\ 3.798 \\ 5.505 \\ -1.760 \\ 6.040 \\ 6.583 \\ -3.757 \\ -5.511 \\ 1.725 \end{bmatrix}$$

with the corresponding worst-case fidelities,

$$\begin{aligned} \min_{\omega \in \Delta_0} \mathcal{F}(\theta_{\Delta_0}) &= 1 - 10^{-15.05} \approx 1.000000 \\ \min_{\omega \in \Delta} \mathcal{F}(\theta_{\Delta_0}) &= 1 - 10^{-4.66} \approx 0.999978 \\ \min_{\omega \in \Delta} \mathcal{F}(\theta_\Delta) &= 1 - 10^{-5.23} \approx 0.999994 \end{aligned}$$

Clearly the control optimized for Δ (dotted red) is only a bit better than the control optimized for Δ_0 , and in addition, the control amplitudes are also extremely close. The main reason

for the closeness of the worst-case fidelities with respect to Δ , and the closeness of the control magnitudes, is that the start-up control, θ_Δ , gives very good performance. And a well-known phenomena with non-convex local optimizers is that solutions often tend to remain near the start-up when the start-up gives good performance [68] which is certainly the case here.

The extreme sensitivity to uncertainty is almost exclusively due to uncertainty in ω_x ; variations in ω_z are not nearly as disruptive. This is due in part to the fact that in our example (5) ω_x is a direct *multiplicative uncertainty* on the control signal. Though small (1% variation), it is nonetheless in a sensitive spot. Gain variation in a classical *open-loop* control also exhibits this kind of sensitivity. Here, in the context of what is considered high performance for quantum computing, the sensitivity is extreme. To see the specific source we follow the procedure presented in [39]. First set $\omega_x = 1 + \tilde{\omega}_x$, $|\tilde{\omega}_x| \leq 0.01$. Consequently, a variation in ω_x about $\omega_x = 1$ is equivalent to a perturbation of $\theta \rightarrow \theta + \tilde{\omega}_x \theta$. This gives rise to the second order Taylor series fidelity approximation,

$$\begin{aligned} \mathcal{F}(\theta, 1 + \tilde{\omega}_x, \omega_z) &= \mathcal{F}(\theta + \tilde{\omega}_x \theta, 1, \omega_z) \\ &\approx \mathcal{F}(\theta, 1, \omega_z) + \tilde{\omega}_x \theta^T \nabla_\theta \mathcal{F}(\theta, 1, \omega_z) \\ &\quad + (\tilde{\omega}_x^2 / 2) \theta^T \nabla_\theta^2 \mathcal{F}(\theta, 1, \omega_z) \theta \end{aligned}$$

In our examples, the Hessian $\nabla_\theta^2 \mathcal{F}(\theta, 1, \omega_z)$ is negative semi-definite, and in all cases the Hessian term dominates the gradient term. Although not shown, when evaluating the fidelity of any control θ_{Δ_0} over all uncertainty in ω_z and with $|\tilde{\omega}_x| \leq 0.01$, we get values of fidelity that coincide almost exactly with points on the tradeoff curve along the dashed blue plot.

Another aspect revealed from the tradeoff curves is seen more readily in Fig. 3, which shows a few samples from the tradeoffs. Although visibly it is difficult to distinguish θ_Δ in Fig. 3(a) from θ_{Δ_0} in Fig. 3(b), the fidelity surfaces are quite different. To some extent the opposite is true in Figs. 3(c-d) where the control magnitude differences are small but visible whereas the fidelity surfaces are almost the same, and clearly not so good for robustness. Table III summarizes some of the key features. In (a) the worst-case is slightly better than in (b) whereas in (b) the average is slightly better than in (a). However, the somewhat central region in (b) where fidelity error is in the range of 10^{-7} is fairly large, suggesting that if the system (5) were designed differently we could have this much improved performance. So although in (b) the worst-case is worse than in (a) – although not so much worse – jointly con-

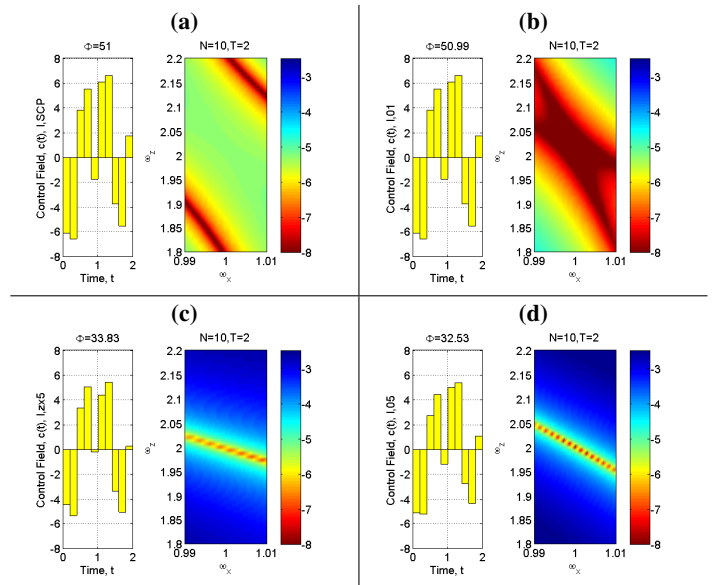


FIG. 3: Robust control pulses and fidelity errors: (a) Start-up control optimized for Δ (15) with $\Phi[c] < \infty$ (no fluence constraint). (b) Control optimized for no uncertainty Δ_0 (18) with $\Phi[c] < \infty$. (c) Control optimized for Δ (15) with $\Phi[c] \leq 33.83$. (d) Control optimized for Δ_0 (18) with $\Phi[c] \leq 32.57$.

sidering system design along with control can bring in unforeseen possibly serendipitous designs. However, we also see from (c-d) that control constraints can quickly drive the design out of the “sweet spot.” Under such a fluence constraint would bring the design within reach to be one from Table II, say (for the identity gate) with $T = 2$ and $N = 20$ fluence is 25.43 which is within the constraints in Figs. 3(c-d).

Control constraints	Fluence achieved	$\log_{10}(1 - \mathcal{F})$		
		worst-case	average	best
(a) Δ , $\Phi[c] < \infty$	51.00	-5.23	-5.55	-9.57
(b) Δ_0 , $\Phi[c] < \infty$	50.99	-4.66	-5.78	-15.05
(c) Δ , $\Phi[c] \leq 33.83$	33.83	-2.65	-3.20	-6.94
(d) Δ_0 , $\Phi[c] \leq 32.57$	32.53	-2.34	-2.97	-15.35

TABLE III: Worst-case, average, and best-case fidelity errors for a few selected controls in Fig. 3 with fluence $\Phi[c] = (T/N) \|\theta\|_2^2$.

VI. SUMMARY

Using SCP we have shown that a substantial fidelity robustness is obtainable against uncertainties while simultaneously using limited resources of control amplitude, bandwidth (number of pulses per time interval), and fluence. What is required is a specific knowledge of the range and character of

the uncertainties, a process referred to in the control theory literature as “uncertainty modeling.” Although we have focused on a single example of a single qubit system, it is clear that even for this case there is a very rich variety of design trade-offs between control constraints (*e.g.*, number of pulses, time interval, fluence, magnitude) and the range of system parameters from the underlying physics (*e.g.*, the parameters (ω_x, ω_x) in (5)). Here we examined a 1% variation due to ω_x , which is a multiplicative gain perturbation to the control, and a 10% variation in ω_z , which to some extent is a coarse approximation to environmental uncertainty. The results presented give an indication of what is possible for different values and ranges. For some implementations the physical parameters, and associated ranges, can be “designed” by selecting the material used in the implementation, the circuit layout, *etc.*. Thus a combination of physical design and robust control design could lead to a “sweet spot” amongst the possibilities. One observation which has surfaced in all our robust control examples is the sensitivity to uncertainty in the control implementation, in particular, the relatively small variation in ω_x . This sensitivity, though, should be viewed in the context of Fig. 2 where the fidelity error rises from essentially zero to a value in the

range of 10^{-4} .

SCP is of course not the only approach to finding local solutions to non-convex problems. One advantage is the ease by which the design variable constraints and the uncertainty modeling can be directly incorporated in the local convex optimization step of the algorithm.

The array of results presented here hopefully herald what would be seen in more complex systems which involve multiple qubits, the inclusion of controlled ancilla, the effect of coupling to a bath, and so on. In addition the results also begin to provide an insight into unanticipated control structures. Many of these potentialities are under consideration at present and will be forthcoming.

Acknowledgments We gratefully acknowledge helpful discussions with Kevin Young (SNL-CA), Kaveh Khodjasteh, and Lorenza Viola (Dartmouth College). The authors acknowledge support from the Intelligence Advanced Research Projects Activity (IARPA) via Department of Interior National Business Center contract number D11PC20165[74] and the Laboratory Directed Research and Development program at Sandia National Laboratories under contract DE-AC04-94AL85000.[75]

-
- [1] Alexander Weinmann. *Uncertain Models and Robust Control*. Springer, Wien, 1991.
- [2] Kemin Zhou and John C. Doyle. *Essentials of Robust Control*. Prentice Hall, Englewood Cliffs, NJ, 1998.
- [3] Geir E. Dullerud and Fernando Paganini. *A Course in Robust Control Theory: A Convex Approach*. Springer, New York, 2000.
- [4] Feng Lin. *Robust Control Design: An Optimal Control Approach*. Wiley, Chichester, UK, revised edition, 2007.
- [5] Aziz Belmiloudi. *Stabilization, Optimal and Robust Control: Theory and Applications in Biological and Physical Sciences*. Springer, London, UK, 2008.
- [6] Genichi Taguchi, Rajesh Jugulum, and Shin Taguchi. *Computer-Based Robust Engineering: Essential For DFSS*. ASQ Quality Press, Milwaukee, 2004.
- [7] Aharon Ben-Tal, Laurent El Ghaoui, and Arkadi Nemirovski. *Robust Optimization*. Princeton University Press, Princeton, NJ, 2009.
- [8] Evan M. Fortunato, Marco A. Pravia, Nicolas Boulant, Grum Teklemariam, Timothy F. Havel, and David G. Cory. Design of strongly modulating pulses to implement precise effective hamiltonians for quantum information processing. *J. Chem. Phys.*, 116(17):7599–7606, 2002.
- [9] Marco A. Pravia, Nicolas Boulant, Joseph Emerson, Amro Farid, Evan M. Fortunato, Timothy F. Havel, R. Martinez, and David G. Cory. Robust control of quantum information. *J. Chem. Phys.*, 119(19):9993–10001, 2003.
- [10] N. Boulant, J. Emerson, T. F. Havel, D. G. Cory, and S. Furuta. Incoherent noise and quantum information processing. *J. Chem. Phys.*, 121(7):2955–2961, 2004.
- [11] Michael Henry, Alexey Gorshkov, Yaakov Weinstein, Paola Cappellaro, Joseph Emerson, Nicolas Boulant, Jonathan Hodges, Chandrasekhar Ramanathan, Timothy Havel, Rudy Martinez, and David Cory. Signatures of incoherence in a quantum information processor. *Quantum Inf. Process.*, 6(6):431–444, 2007.
- [12] Troy W. Borneman, Martin D. Hürlimann, and David G. Cory. Application of optimal control to CPMG refocusing pulse design. *J. Magn. Reson.*, 207(2):220–233, December 2010.
- [13] Janus Wesenberg and Klaus Mølmer. Robust quantum gates and a bus architecture for quantum computing with rare-earth-ion-doped crystals. *Phys. Rev. A*, 68(1):012320, Jul 2003.
- [14] Janus H. Wesenberg. Designing robust gate implementations for quantum-information processing. *Phys. Rev. A*, 69(4):042323, Apr 2004.
- [15] Ingela Roos and Klaus Mølmer. Quantum computing with an inhomogeneously broadened ensemble of ions: Suppression of errors from detuning variations by specially adapted pulses and

- coherent population trapping. *Phys. Rev. A*, 69(2):022321, Feb 2004.
- [16] Thomas E. Skinner, Timo O. Reiss, Burkhard Luy, Navin Khaneja, and Steffen J. Glaser. Application of optimal control theory to the design of broadband excitation pulses for high-resolution NMR. *J. Magn. Reson.*, 163(1):8–15, 2003.
- [17] Kyril Kobzar, Thomas E. Skinner, Navin Khaneja, Steffen J. Glaser, and Burkhard Luy. Exploring the limits of broadband excitation and inversion pulses. *J. Magn. Reson.*, 170(2):236–243, 2004.
- [18] Kyril Kobzar, Burkhard Luy, Navin Khaneja, and Steffen J. Glaser. Pattern pulses: design of arbitrary excitation profiles as a function of pulse amplitude and offset. *J. Magn. Reson.*, 173(2):229–235, 2005.
- [19] Burkhard Luy, Kyril Kobzar, Thomas E. Skinner, Navin Khaneja, and Steffen J. Glaser. Construction of universal rotations from point-to-point transformations. *J. Magn. Reson.*, 176(2):179–186, 2005.
- [20] Navin Khaneja, Timo Reiss, Cindie Kehlet, Thomas Schulte-Herbrüggen, and Steffen J. Glaser. Optimal control of coupled spin dynamics: design of NMR pulse sequences by gradient ascent algorithms. *J. Magn. Reson.*, 172(2):296–305, 2005.
- [21] Thomas E. Skinner, Kyril Kobzar, Burkhard Luy, M. Robin Bendall, Wolfgang Bermel, Navin Khaneja, and Steffen J. Glaser. Optimal control design of constant amplitude phase-modulated pulses: Application to calibration-free broadband excitation. *J. Magn. Reson.*, 179(2):241–249, 2006.
- [22] N. Timoney, V. Elman, S. Glaser, C. Weiss, M. Johanning, W. Neuhauser, and Chr. Wunderlich. Error-resistant single-qubit gates with trapped ions. *Phys. Rev. A*, 77(5):052334, 2008.
- [23] Navin Khaneja, Cindie Kehlet, Steffen J. Glaser, and Niels Chr. Nielsen. Composite dipolar recoupling: Anisotropy compensated coherence transfer in solid-state nuclear magnetic resonance. *J. Chem. Phys.*, 124(11):114503, 2006.
- [24] Brent Pryor and Navin Khaneja. Fourier decompositions and pulse sequence design algorithms for nuclear magnetic resonance in inhomogeneous fields. *J. Chem. Phys.*, 125(19):194111, 2006.
- [25] Jr-Shin Li and Navin Khaneja. Control of inhomogeneous quantum ensembles. *Phys. Rev. A*, 73(3):030302, Mar 2006.
- [26] Philip Owrutsky and Navin Khaneja. Control of inhomogeneous ensembles on the Bloch sphere. *Phys. Rev. A*, 86(2):022315, Aug 2012.
- [27] Justin Ruths and Jr-Shin Li. A multidimensional pseudospectral method for optimal control of quantum ensembles. *J. Chem. Phys.*, 134(4):044128, 2011.
- [28] Justin Ruths and Jr-Shin Li. Optimal control of inhomogeneous ensembles. 2011.
- [29] Matthias Steffen and Roger H. Koch. Shaped pulses for quantum computing. *Phys. Rev. A*, 75(6):062326, Jun 2007.
- [30] M. J. Testolin, C. D. Hill, C. J. Wellard, and L. C. L. Hollenberg. Robust controlled-not gate in the presence of large fabrication-induced variations of the exchange interaction strength. *Phys. Rev. A*, 76(1):012302, Jul 2007.
- [31] Brian Mischuck, Ivan H. Deutsch, and Poul S. Jessen. Coherent control of atomic transport in spinor optical lattices. *Phys. Rev. A*, 81(2):023403, Feb 2010.
- [32] Brian E. Mischuck, Seth T. Merkel, and Ivan H. Deutsch. Control of inhomogeneous atomic ensembles of hyperfine qubits. *Phys. Rev. A*, 85(2):022302, Feb 2012.
- [33] B. Khani, S. T. Merkel, F. Motzoi, Jay M. Gambetta, and F. K. Wilhelm. High-fidelity quantum gates in the presence of dispersion. *Phys. Rev. A*, 85(2):022306, Feb 2012.
- [34] Matthew D. Grace, Jason M. Dominy, Wayne M. Witzel, and Malcolm S. Carroll. Optimized pulses for the control of uncertain qubits. *Phys. Rev. A*, 85(5):052313, May 2012.
- [35] Xin Wang, Lev S. Bishop, J. P. Kestner, Edwin Barnes, Kai Sun, and S. Das Sarma. Composite pulses for robust universal control of singlet-triplet qubits. *Nat. Commun.*, 3(8):997, August 2012.
- [36] Christopher Stihl, Benedikt Fauseweh, Stefano Pasini, and Götz S. Uhrig. Modulated pulses compensating classical noise. *quant-ph/ArXiv:1210.4311*, 2012.
- [37] Todd J. Green, Jarrah Sastrawan, Hermann Uys, and Michael J. Biercuk. Arbitrary quantum control of qubits in the presence of universal noise. *quant-ph/ArXiv:1211.1163*, 2012.
- [38] Gregory Quiroz and Daniel A. Lidar. Optimized dynamical decoupling via genetic algorithms. *quant-ph/ArXiv:1210.5538*, 2012.
- [39] Constantin Brif, Matthew D. Grace, Kevin C. Young, David L. Hocker, Katharine W. Moore, Tak-San Ho, and Herschel Rabitz. Protecting quantum gates from control noise. In *QEC11: Second International Conference on Quantum Error Correction*, Los Angeles, CA, December 2011. Available online at <http://qserver.usc.edu/qec11/program.html>.
- [40] A. Ben-Tal and A. Nemirovski. Robust convex optimization. *Mathematics of Operations Research*, 23(4):769–805, November 1998.
- [41] Aharon Ben-Tal and Arkadi Nemirovski. Robust optimization — methodology and applications. *Math. Program., Ser. B*, 92(3):453–480, 2002.
- [42] Laurent El Ghaoui, Francois Oustry, and Hervé Lebret. Robust solutions to uncertain semidefinite programs. *SIAM J. Optim.*, 9(1):33–52, 1998.
- [43] Dimitris Bertsimas and Melvyn Sim. Tractable approximations to robust conic optimization problems. *Math. Program., Ser. B*, 107(1):5–36, 2006.
- [44] G. C. Calafiore and M. C. Campi. The scenario approach to robust control design. *IEEE Trans. Autom. Control*, 51(5):742–753, May 2006.
- [45] S. A. Vorobyov, A. B. Gershman, and Zhi-Quan Luo. Robust adaptive beamforming using worst-case performance optimiza-

- tion: a solution to the signal mismatch problem. *IEEE Trans. Signal Process.*, 51(2):313–324, Feb 2003.
- [46] R. G. Lorenz and S. P. Boyd. Robust minimum variance beamforming. *IEEE Trans. Signal Process.*, 53(5):1684–1696, May 2005.
- [47] B. Rustem and M. Howe. *Algorithms for Worst-Case Design and Applications to Risk Management*. Princeton University Press, Princeton, NJ, 2002.
- [48] Laurent El Ghaoui, Maksim Oks, and Francois Oustry. Worst-case value-at-risk and robust portfolio optimization: A conic programming approach. *Operations Research*, 51(4):543–556, July/August 2003.
- [49] Gert R.G. Lanckriet, Laurent El Ghaoui, Chiranjib Bhattacharyya, and Michael I. Jordan. A robust minimax approach to classification. *J. Mach. Learn. Res.*, 3:555–582, Mar 2003.
- [50] Y. Zhang. General robust-optimization formulation for nonlinear programming. *J. Optimiz. Theory Applic.*, 132:111–124, 2007.
- [51] Almir Mutapcic and Stephen Boyd. Cutting-set methods for robust convex optimization with pessimizing oracles. *Optimization Methods Software*, 24(3):381–406, June 2009.
- [52] Dimitris Bertsimas, Omid Nohadani, and Kwong Meng Teo. Robust optimization for unconstrained simulation-based problems. *Operations Research*, 58(1):161–178, January/February 2010.
- [53] Dimitris Bertsimas, Omid Nohadani, and Kwong Meng Teo. Nonconvex robust optimization for problems with constraints. *J. Computing*, 22(1):44–58, 2010.
- [54] Almir Mutapcic, Stephen Boyd, Ardavan Farjadpour, Steven G. Johnson, and Yehuda Avniel. Robust design of slow-light tapers in periodic waveguides. *Engineering Optimization*, 41(4):365–384, April 2009.
- [55] Ardavan Oskooi, Almir Mutapcic, Susumu Noda, J. D. Joannopoulos, Stephen P. Boyd, and Steven G. Johnson. Robust optimization of adiabatic tapers for coupling to slow-light photonic-crystal waveguides. *Opt. Express*, 20(19):21558–21575, September 2012.
- [56] J. Zhang and R. L. Kosut. Robust design of quantum potential profile for electron transmission in semiconductor nanodevices. In *2007 European Control Conference*, Kos, Greece, July 2007.
- [57] Herschel A. Rabitz, Michael M. Hsieh, and Carey M. Rosenthal. Quantum optimally controlled transition landscapes. *Science*, 303(5666):1998–2001, Mar 2004.
- [58] Raj Chakrabarti and Herschel Rabitz. Quantum control landscapes. *Int. Rev. Phys. Chem.*, 26(4):671–735, Oct 2007.
- [59] Constantin Brif, Raj Chakrabarti, and Herschel Rabitz. Control of quantum phenomena: past, present and future. *New J. Phys.*, 12(7):075008, July 2010.
- [60] Constantin Brif, Raj Chakrabarti, and Herschel Rabitz. Control of quantum phenomena. In S. A. Rice and A. R. Dinner, editors, *Adv. Chem. Phys.*, volume 148, pages 1–76. Wiley, New York, 2012.
- [61] Herschel Rabitz, Michael Hsieh, and Carey Rosenthal. Landscape for optimal control of quantum-mechanical unitary transformations. *Phys. Rev. A*, 72(5):052337, 2005.
- [62] Michael Hsieh and Herschel Rabitz. Optimal control landscape for the generation of unitary transformations. *Phys. Rev. A*, 77(4):042306, Apr 2008.
- [63] Tak-San Ho, Jason Dominy, and Herschel Rabitz. Landscape of unitary transformations in controlled quantum dynamics. *Phys. Rev. A*, 79(1):013422, Jan 2009.
- [64] Katharine W. Moore, Raj Chakrabarti, Gregory Riviello, and Herschel Rabitz. Search complexity and resource scaling for the quantum optimal control of unitary transformations. *Phys. Rev. A*, 83(1):012326, Jan 2011.
- [65] Katharine W Moore and Herschel Rabitz. Exploring constrained quantum control landscapes. *J. Chem. Phys.*, 137(13):134113, 2012.
- [66] K. Schittkowski and C. Zillober. Sequential convex programming methods. In K. Marti and P. Kail, editors, *Stochastic Programming*, volume 423 of *Lecture Notes in Economics and Mathematical Systems*. Springer, 1995.
- [67] Stephen P. Boyd. Ee364b, lecture notes. Available online at <http://www.stanford.edu/~boyd>.
- [68] S. Boyd and L. Vandenberghe. *Convex Optimization*. Cambridge University Press, Cambridge, UK, 2004.
- [69] J. Lofberg. YALMIP: A Toolbox for Modeling and Optimization in MATLAB. In *Proceedings of the CACSD Conference*, Taipei, Taiwan, 2004.
- [70] CVX Research Inc. CVX: Matlab software for disciplined convex programming, version 2.0 beta. <http://cvxr.com/cvx>, September 2012.
- [71] M. Grant and S. Boyd. Graph implementations for nonsmooth convex programs. In V. Blondel, S. Boyd, and H. Kimura, editors, *Recent Advances in Learning and Control*, Lecture Notes in Control and Information Sciences, pages 95–110. Springer-Verlag Limited, 2008. http://stanford.edu/~boyd/graph_dcp.html.
- [72] K. C. Toh, R. H. Tutuncu, and M. J. Todd. SDPT3: MATLAB software for semidefinite-quadratic-linear programming. 2004. <http://www.math.nus.edu.sg/~mattokc/sdpt3.html>.
- [73] J. F. Sturm. Using SeDuMi 1.02, a MATLAB toolbox for optimization over symmetric cones. *Optimization Methods and Software*, 11-12:625–653, 1999. Special issue on Interior Point Methods; available from <http://fewcal.kub.nl/sturm/software/sedumi.html>.
- [74] The U.S. Government is authorized to reproduce and distribute reprints for Governmental purposes notwithstanding any copyright annotation thereon. Disclaimer: The views and conclusions contained herein are those of the authors and should not be interpreted as necessarily representing the official poli-

cies or endorsements, either expressed or implied, of IARPA, DoI/NBC, or the U.S. Government.

[75] Sandia Corporation is a wholly owned subsidiary of Lockheed Martin Corporation, for the United States Department of Energy's National Nuclear Security Administration

Appendix A: Convex optimization

The convex optimization step in the SCP algorithm can be equivalently expressed as,

$$\begin{aligned} & \text{maximize } f_0 \\ & \text{subject to } f_i + g_i^T \tilde{\theta} \geq f_0, \quad i = 1, \dots, L \\ & \quad \theta + \tilde{\theta} \in \Theta, \quad \tilde{\theta} \in \tilde{\Theta}_{\text{trust}} \end{aligned} \quad (\text{A1})$$

with $f_i = \mathcal{F}(\theta, \delta_i) \in \mathbf{R}$ and $g_i = \nabla_{\theta} \mathcal{F}(\theta, \delta_i) \in \mathbf{R}^N$. The optimization variables are now both $\tilde{\theta} \in \mathbf{R}^N$ and f_0 . If both Θ and $\tilde{\Theta}_{\text{trust}}$ bound their respective elements in a ‘‘box’’ in \mathbf{R}^N , then (A1) is a *linear program*.

The Hessian can be included by using its negative semidefinite part, $R_i = -[\nabla_{\theta}^2 \mathcal{F}(\theta, \delta_i)]_-$ where $[\cdot]_-$ retains only the negative eigenvalues of the Hessian, all others set to zero. Then the worst-case fidelity constraint becomes,

$$f_i + g_i^T \tilde{\theta} - (1/2) \tilde{\theta}^T R_i \tilde{\theta} \geq f_0, \quad i = 1, \dots, L$$

Each of these inequalities is equivalent to a linear-matrix-inequality (LMI) in the variables $(\tilde{\theta}, f_0)$ [68]. The optimization step in SCP is now given by the semidefinite program,

$$\begin{aligned} & \text{maximize } f_0 \\ & \text{subject to } \begin{bmatrix} f_i - f_0 - g_i^T \tilde{\theta} & \tilde{\theta}^T / \sqrt{2} \\ \tilde{\theta} / \sqrt{2} & R_i^{\#} \end{bmatrix} \geq 0, \quad i = 1, \dots, L \\ & \quad \theta + \tilde{\theta} \in \Theta, \quad \tilde{\theta} \in \tilde{\Theta}_{\text{trust}} \end{aligned} \quad (\text{A2})$$

with $R_i^{\#}$ the pseudo-inverse of R_i .

The optimization problems (A1) and (A2) are now in standard forms suitable for use with existing software especially developed for these classes of convex optimization. In particular, YALMIP [69] and CVX [70, 71] are convex compilers compatible with MATLAB. Using these software tools makes it very easy to code the convex optimization problems almost exactly as expressed mathematically. These compilers call convex solvers such as SDPT-3 [72] and SeDuMi [73] which have been developed and in use for many years, and as a result are generally efficient and reliable. There are limits imposed by both memory and speed for a particular problem instance and computer platform. In these cases it is often necessary to use, if available, or develop as necessary, specialized versions

with modifications that take into account the specific underlying structure of the problem.

Appendix B: Signal generation

In general the control $c(t, \theta)$ is the output of a signal generation device. As an example, consider the control generated from a system with time constant τ and piece-wise-constant commands:

$$\begin{aligned} \dot{c}(t, \theta) &= (1/\tau)(\bar{c}(t, \theta) - c(t, \theta)), \quad c(0) = 0 \\ \bar{c}(t, \theta) &= \theta_k, \quad (k-1)T/N \leq t < kT/N, \quad k = 1, \dots, N \end{aligned} \quad (\text{B1})$$

In this case,

$$c(t, \theta) = \sum_{k=1}^N s_k(t) \theta_k = s(t)^T \theta, \quad 0 \leq t \leq T \quad (\text{B2})$$

This expression holds for *any* signal generation well represented by known linear dynamics whose input is a sequence of N control commands $\theta_k, k = 1, \dots, N$ at a uniform sampling rate T/N . The linear dynamics are captured in the shape function vector $s(t) \in \mathbf{R}^N$, the elements of which in the above example (B1) are given by $s_k(t) = 1 - e^{-(t-(k-1)T/N)/\tau}$ for $(k-1)T/N \leq t < kT/N$ and $s_k(t) = (1 - e^{(T/N)/\tau})e^{-(t-kT/N)/\tau}$ for $t \geq kT/N$. In the ideal case with very fast dynamics ($\tau \rightarrow \infty$) the control is simply piece-wise-constant over N uniform time intervals of width T/N as given by (6) where the shape functions reduce to piece-wise-constant unit pulses of uniform width T/N . When the dynamics of the control generation device have an appreciable effect on these pulses, the product formula (8) for computing the final time unitary must be replaced by a continuous-time simulation. In our example this would be,

$$i\dot{U} = (c(t, \theta)\omega_x X + \omega_z Z)U, \quad U_0 = I \quad (\text{B3})$$

For any control in the form of (B2), the control constraint sets in Table I form convex sets in θ . For example, the fluence constraint $\Phi[c] = \int_0^T c^2(t, \theta) dt \leq \gamma^2$ is equivalent to $\Phi(\theta) = \theta^T Q \theta \leq \gamma^2$ with $Q = \int_0^T s(t)s(t)^T dt$.

For laser control pulse shaping via a liquid crystal array, the controls are typically both phase and amplitude at each Fourier frequency component of the laser pulse after passing through an optical grating. Ignoring any dynamics in the crystal, the control signal is of the form $c(t) = \sum_{i=1}^K a_i \sin(\omega_i t + \phi_i)$, with known frequencies ω_i and controls (a_i, ϕ_i) . The

control can be equivalently expressed in a form similar to (B2) as,

$$c(t, \theta) = \sum_{i=1}^K s_i(t)^T \theta_i \quad (\text{B4})$$

with multiple shape functions $s_i(t)^T = [\sin(\omega_i t) \ \cos(\omega_i t)]$ and $\theta_i^T = a_i [\cos \phi_i \ \sin \phi_i]$. Since $\|\theta_i\|_2 = a_i$, the magnitude constraint $0 \leq a_i \leq a_{\max}$ brings (B4) again into a convex

set in θ . The phases and amplitudes are easily obtained from any θ so constrained found from SCP. If, however, all the amplitudes are the same, *i.e.*, $a_i = a_0$, and only the phases are controlled, the constraint $\|\theta_i\|_2 \leq a_0$ is a *convex relaxation* [68] of the actual (non-convex) constraint $\|\theta_i\|_2 = a_0$, and hence, SCP will return a local solution to the relaxed problem. Some relaxations can be proven to be optimal; that is not known here, thus a post-optimization analysis is required.